

Comparative Study on Planar-silicon and Nano-silicon Si/PCBM Inorganic-organic Hybrid Junctions

LIU Wei-Feng¹, BIAN Ji-Ming^{1,2}, LUO Ying-Lin¹, QIAO Jian-Kun¹, ZHAO Chun-Yi¹

(1. Key Laboratory of Materials Modification by Laser, Ion and Electron Beams (Ministry of Education), School of Physics and Optoelectronic Technology, Dalian University of Technology, Dalian 116024, China; 2. Key Laboratory of Inorganic Coating Materials, Chinese Academy of Sciences, Shanghai 200050, China)

Abstract: Inorganic-organic heterojunction devices based on organic polymer and inorganic semiconductors has attracted extensive attention for high performance hybrid solar cell applications, due to the combined advantage of high carrier mobility of inorganic semiconductors and easy processing, strong absorption of organic polymers. In this study, both planar-Si and nano-Si were combined with spin-coated [6, 6]-phenyl C61-butyric acid methyl ester (PCBM) organic film to form Si/PCBM inorganic/organic hybrid junctions. A comparative study was performed through quantitative electrical analysis of planar-Si/PCBM and nano-Si/PCBM, respectively. In general, both devices exhibited a rectifying diode-like behavior. However, a higher turn-on voltage and smaller current density were observed from nano-Si/PCBM junctions, which was in contradiction with the expectation from the view of junction area. The corresponding mechanisms were further investigated with measurements of impedance spectroscopy (IS). Our results indicated that this abnormal electrical characteristic of nano-Si/PCBM compared with normal p-n junction was highly associated with the parasitic effects caused by the defect states at the junction interface.

Key words: inorganic-organic heterojunction; nano-Si/PCBM; impedance spectroscopy

Inorganic-organic heterojunction devices are of great importance in organic electronic devices, and their potential applications include light-emitting devices, solar cells and other electronic devices^[1-2]. Research focused on hybrid solar cells based on organic polymer and inorganic semiconductors has led to recent realization of its power conversion efficiency up to 5.13%^[3-5]. Inorganic-organic heterojunction solar cells combine the high carrier mobility of inorganic semiconductors and easy processing, strong absorption of organic polymers^[6]. The most popular active material system consists of inorganic-organic heterojunction that is formed by a p-type inorganic semiconductor such as Si, with an n-type organic semiconductor (electron acceptor) such as methanofullerene derivatives (PCBM). In addition, inorganic/organic hybrid junction devices based nano-surface present great potential for low-cost large area optoelectronic devices, which will benefit from large area junction induced by nano-surface treatment^[7]. Based on this ideation, recently, some groups have improved efficiency of solar cells by using hybrid

junction devices with nano-junction interface. Boucle, *et al*^[8] improved the efficiency of inorganic-organic heterojunction solar cells by optimizing density and length of nanowires to decrease charger combination. Moreover, Beek, *et al* obtained a higher efficiency by enlarging junction area^[9]. In general, conventional measurements, such as *I-V* and *C-V*, were employed to characterize the property of p-n junction. However, the electronic characters of inorganic/organic hybrid junction devices with nano-junction interface were seldom researched by impedance spectroscopy (IS) measurements. Impedance spectroscopy measurements could reflect changes of resistance and capacitance in heterojunctions along with extra bias voltage^[10]. Therefore, IS techniques was believed to be powerful method to elucidate the corresponding mechanisms of Si based inorganic/organic hybrid junctions.

In this comparative study, the performance of nano-Si/PCBM heterojunction and planar-Si/PCBM heterojunction was quantitatively analyzed. The corresponding mechanisms were further investigated and elucidated based on

Received date: 2014-08-14; **Modified date:** 2014-11-16; **Published online:** 2014-12-10

Foundation item: Natural Science Foundation of Liaoning Province (2013020095); Fundamental Research Funds for the Central Universities (DUT13LK02, DUT13LAB12)

Biography: LIU Wei-Feng(1976–), male, lecturer. E-mail: lwf008@163.com

Corresponding author: BIAN Ji-Ming, associate professor. E-mail: jmbian@dlut.edu.cn

the measurements of IS.

1 Experimental procedure

In this study, nano-Si/PCBM and planar-Si/PCBM heterojunctions were prepared as shown in Fig. 1. The P-type (100) nano-Si and planar-Si with the resistivity of 1–3 $\Omega\cdot\text{cm}$ were used as the substrates in the nano-Si/PCBM and planar-Si/PCBM structure, respectively. As for nano-Si, Si nanowires (NWs) array was formed on the surface of the Si wafer by means of a developed silver-catalyzed electroless etching process at 20 $^{\circ}\text{C}$ for 40 s in an etching solution with the volume ratio of deionization water/HF (49%)/ H_2O_2 (30%)/ AgNO_3 (0.1 mol/L)=8 : 2 : 1 : 1. The Si NWs were distributed on the Si surface, the diameter varied from 30 to 150 nm, and the length varied from 50 to 600 nm. Details of the etching process can be found in our previous research work^[11]. Prior to fabricating the heterojunctions, Al back electrodes with about 100 nm thickness were evaporated on the nano-Si and planar-Si by thermal evaporation in a vacuum chamber (base pressure of 5×10^{-4} Pa), and then annealed at 450 $^{\circ}\text{C}$ for 5 min to form Ohm contact. To prepare uniform PCBM film on the substrates, we applied spin coating technology. PCBM (15 mg/mL) was dissolved in chlorobenzene at 140 $^{\circ}\text{C}$ with stirring for

one hour to be used for spin coating solution. The organic PCBM layer was spin-coated on the nano-Si and planar-Si substrate with revolution of 1000 r/min for 40 s. Due to difference of adhesion coefficient between nano-Si substrates and planar-Si substrates, the thickness was about 200 nm and 600 nm, respectively. After spin-coating, the samples were kept at 80 $^{\circ}\text{C}$ for 30 min to remove the remaining solvent. Then 100 nm Al layer as a top electrode was deposited by thermal evaporation in a vacuum chamber (base pressure of 5×10^{-4} Pa) through a shadow mask.

The morphology and structures of the samples were characterized with scanning electron microscopy (NOVA NanoSEM 450). The current-voltage (I - V) characteristic was measured by current-voltage source (Keithley 2611 A). Impedance spectrum (IS) of all the samples were characterized with impedance spectrum analyzer (Zahner IM6e) in the darkness. Both of the samples were measured under a range of bias voltages from 0 to 0.5 V.

2 Results and discussion

2.1 Current-voltage (I - V) measurement

To investigate the electrical properties of Si/PCBM structure, I - V measurement was used to study both devices. Figure 2 represents the typical I - V characteristic

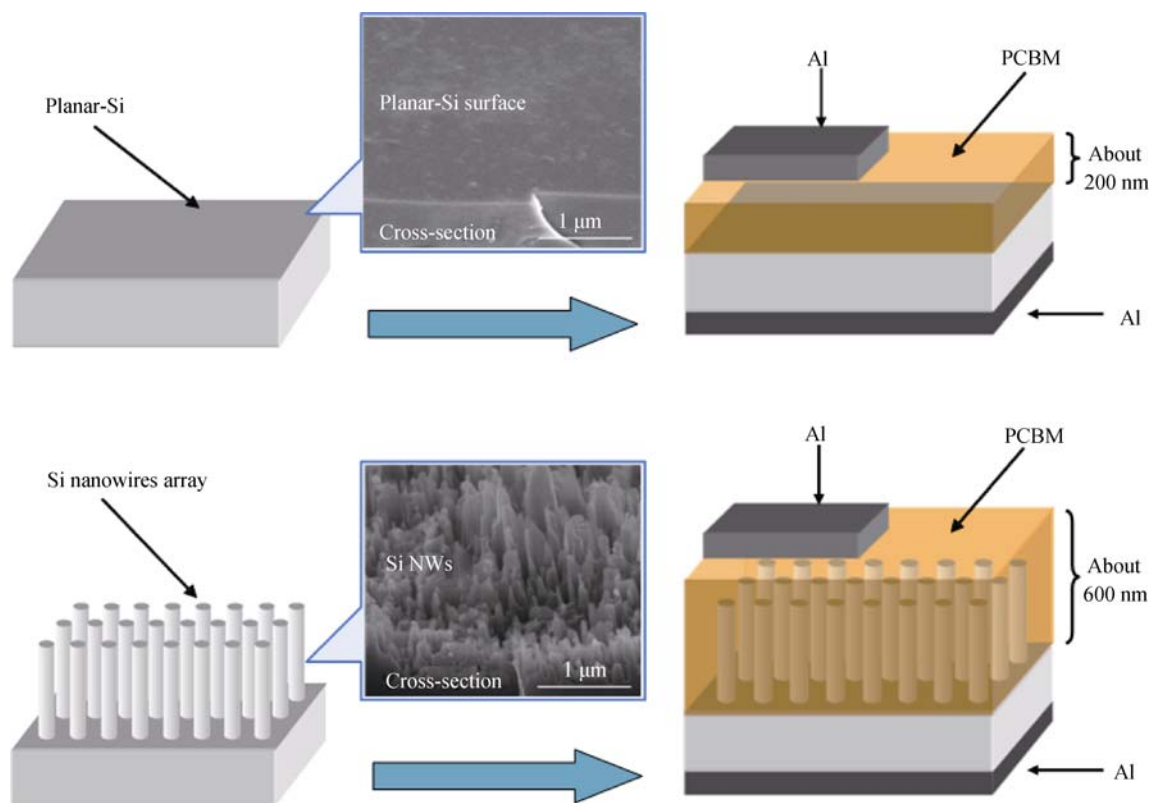


Fig. 1 Three-dimensional schematic diagrams of planar-Si/PCBM and nano-Si/PCBM inorganic/organic, the middle is cross-sectional SEM images of planar-Si and nano-Si

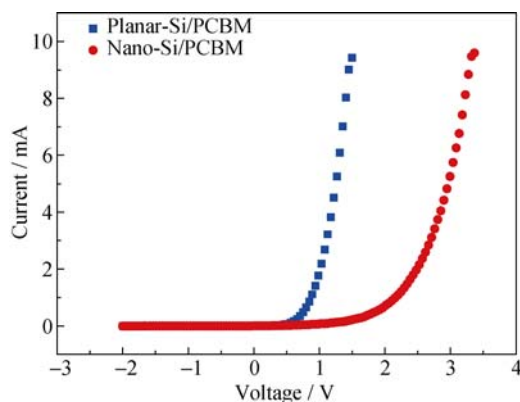


Fig. 2 I - V curves of the planar-Si/PCBM and nano-Si/PCBM inorganic/organic heterojunctions

for Si/PCBM heterojunction devices at room temperature (RT). In general, both the devices exhibited a rectifying diode-like behavior as expected from the p-Si/n-PCBM nature, while the turn-on voltage for planar-Si/PCBM and nano-Si/PCBM was observed to be 0.9 V and 2.5 V, respectively. Remarkable difference can be observed from the I - V characteristic for both devices. In theory, the current of device with large junction area is higher than that of device with small junction area, the turn-on voltages are almost not changed. I - V characteristic for nano-Si/PCBM heterojunction device is expected to show higher current owing to large surface-to-volume ratio. Compared to planar-Si/PCBM, nano-Si/PCBM do not exhibit improved rectifying behavior with high current as expected. However, the higher turn-on voltage of 2.5 V was obtained for nano-Si/PCBM device. Since Si and PCBM remain unaltered, the phenomenon of turn-on voltage becomes large which disagrees with the band theory of semiconductor materials. This nonideal behavior is often attributed to defect states at junction interface or variations in interface composition^[12-13]. However, the deep mechanism and causes of the changes in electrical characteristics for nano-Si/PCBM device still needs further study. Then, the characteristics of defect states at junction interface and their influence factors on the electrical characteristics were analyzed based on the IS measurement.

2.2 Impedance spectroscopy

In order to further investigate the influence of defect states and improve the performance of inorganic-organic heterojunction devices, a better understanding of the interface information is required^[14]. IS has been extensively used to characterize inorganic-organic semiconductor devices. The IS technique consists in the measurement of electrical impedance Z as a function of the frequency of the input signal over a wide frequency range. The collected data may be visualized as a Nyquist diagram or cole-cole plot, represented by the imaginary component Z''

of the impedance as a function of Z' the real component^[15]. The cole-cole plots of Al/PCBM/Si/Al at several dc bias voltages were seen in Fig. 3(a) and 3(b). From the plots, we could find a series of integral semicircles due to the junction of planar-Si/PCBM and nano-Si/PCBM. In addition, we could find the diameters of semicircles apparently decrease with the increasing applied dc bias. The strong dependence of the impedance with the bias indicates the presence of a depletion layer in the samples with a resistance decreasing with increasing bias. Furthermore, the impedance spectra in Fig. 3(a) and 3(b) are not perfect semicircles. The arcs are compressed, with centers of radius below the Re (Z) axis. This behavior is known to

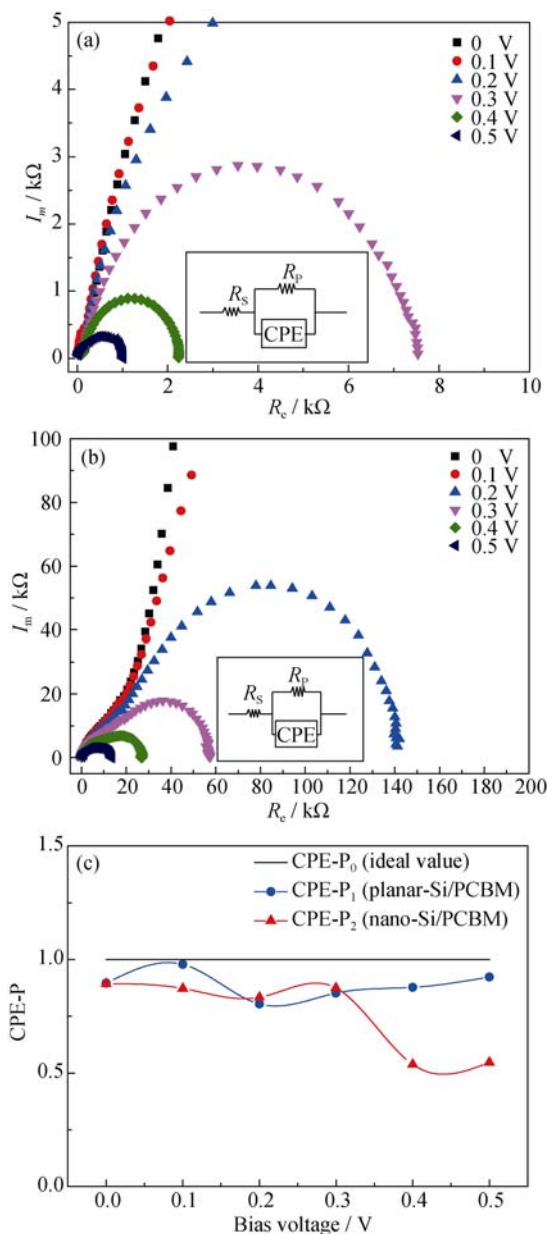


Fig. 3 The cole-cole plots of planar-Si/PCBM heterojunction(a) and nano-Si/PCBM heterojunction with the equivalent electrical circuit (inset), (b) and their CPE-P values (CPE-P₁ and CPE-P₂, respectively) against the ideal value (c)

Table 1 Summary of the circuit parameters obtained from the software of Z-view

Bias/V	planar-Si/PCBM heterojunction			nano-Si/PCBM heterojunction		
	$R_{p1}/M\Omega$	$CPE-T_1/F$	$CPE-P_1$	$R_{p2}/M\Omega$	$CPE-T_2/F$	$CPE-P_2$
0	0.425000	3.87×10^{-8}	0.89571	3.390000	3.52×10^{-8}	0.89312
0.1	0.056518	4.22×10^{-8}	0.97869	0.646970	4.12×10^{-8}	0.87240
0.2	0.023646	3.61×10^{-8}	0.80414	0.132260	5.96×10^{-8}	0.83301
0.3	0.007371	2.34×10^{-8}	0.85180	0.043541	6.47×10^{-8}	0.87478
0.4	0.001279	1.86×10^{-8}	0.87707	0.030387	3.41×10^{-8}	0.53783
0.5	0.000820	1.39×10^{-8}	0.92249	0.014757	2.92×10^{-8}	0.54729

result from inhomogeneities in the electrical properties of the measured interface. Such inhomogeneities include roughness and interface states induced by defects.

An equivalent electrical circuit was created to further investigate the mechanism behind the observed behavior. Because of the existence of large defect states, we select the Constant Phase Element (CPE) instead of traditional C, and the equivalent electrical circuit is shown in Fig. 3(a) and 3(b). The impedance of the CPE is defined as

$$Z(\omega) = 1/(Q\omega t)^\alpha \quad (1)$$

$$CPE-P=\alpha \quad (2)$$

$$CPE-T=Q \quad (3)$$

Where α (CPE-P) is a fitting parameter with a value between 0 and 1, ω is the frequency^[16]. When α is 1, the element is an ideal capacitor with the capacitance equal to Q (CPE-T). As the homogeneity of the interface decreases, α (CPE-P) is expected to deviate further from 1. Figure 3(a) and 3(b) show that the impedance data were fitted as the equivalent circuit. Circuit parameters were obtained from the software of Z-view, and the parameters are summarized in Table 1. In the process of fitting, a series of second semicircles were neglected, which are the reflection of Schottky barrier. In addition, fitted R_s values were negligible for the heterojunctions; their values are not included in the table. From the table, we could find that under the same bias voltage, the R_p of nano-Si/PCBM are one order of magnitude larger than the planar-Si/PCBM due to the large defect states in the nanowires array. Furthermore, both $CPE-P_1$ and $CPE-P_2$ with bias voltage are plotted in Fig. 3(c). $CPE-P_2$ deviates from 1 more than $CPE-P_1$ along with the range of bias voltages, which indicates that large defect states occupy the energy level and increasingly impact on the performance of devices. This abnormal electrical characteristic of nano-Si/PCBM compared with normal p-n junction was highly associated with the parasitic effects caused by the defect states at the junction interface. As a result, the nano-Si/PCBM did not exhibit improved rectifying behavior with high current compared to planar-Si/PCBM.

3 Conclusions

In summary, a comparative study was performed through quantitative analysis of planar-Si/PCBM and nano-Si/PCBM, respectively. In general, both devices exhibited a rectifying diode-like behavior. However, a higher turn-on voltage and smaller current were observed from nano-Si/PCBM junctions, which was in contradiction with the expectation from the view of junction area. The corresponding mechanisms were further investigated with measurements of impedance spectroscopy (IS). The value of $CPE-P_2$ deviates from the ideal more than the $CPE-P_1$ with the bias voltages increasing in the measurement of IS.

References:

- [1] RIEDE M, UHRICH C, WIDMER J, *et al.* Efficient organic tandem solar cells based on small molecules. *Adv. Funct. Mater.*, 2011, **21(16)**: 3019–3028.
- [2] DONG X W, PAN Q Y, HUANG YAN, *et al.* Novel organic-inorganic photochromic film based on mono-vacant Keggin-type polyoxometalates. *J. Inorg. Mater.* 2007, **22(2)**: 369–372.
- [3] LIU C Y, HOLMAN Z C, KORTSHAGEN U R, *et al.* Hybrid solar cells from P3HT and silicon nanocrystals. *Nano Lett.*, 2009, **9(1)**: 449–452.
- [4] LIU C Y, HOLMAN Z C, KORTSHAGEN U R, *et al.* Optimization of Si NC/P3HT hybrid solar cells. *Adv. Funct. Mater.*, 2010, **20(13)**: 2157–2164.
- [5] CHANG J A, RHEE J H, IM S H, *et al.* High-performance nanostructured inorganic organic heterojunction solar cells. *Nano Lett.*, 2010, **10(7)**: 2609–2612.
- [6] HUYNH W U, DITTMER J J, ALIVISATOS A P, *et al.* Hybrid nanorod-polymer solar cells. *Science*, 2002, **295(5564)**: 2425–2427.
- [7] KOLNENKAMP R, WORD R C, GODINEZ M, *et al.* Ultraviolet

- electroluminescence from ZnO/polymer heterojunction light-emitting diodes. *Nano Lett.*, 2005, **5**(10): 2005–2008.
- [8] BOUCLE J, SNAITH H J, GREENHAM N C, *et al.* Simple approach to hybrid polymer porous metal oxide solar cells from solution-processed ZnO nanocrystals. *J. Phys. Chem. C*, 2010, **114**(8): 3664–3674.
- [9] BEEK W J E, WIENK M M, JANSSEN R A J, *et al.* Efficient hybrid solar cells from zinc oxide nanoparticles and a conjugated polymer. *Advanced Materials*, 2004, **16**(12): 1009–1013.
- [10] ZHANG K, LI J, LI Q, *et al.* Improvement on electrochemical performance by electrodeposition of polyaniline nanowires at the top end of sulfur electrode. *Appl. Surf. Sci.*, 2013, **285**(10): 900–906.
- [11] LIU W F, BIAN J M, ZHAO Z C, *et al.* Low temperature surface passivation of black silicon solar cells by high-pressure O₂ thermal oxidation. *ECS Solid State Lett.*, 2013, **2**(4): Q17–Q20.
- [12] WU W, BIAN J M, SUN J C, *et al.* A comparative study of ZnO film and nanorods for ZnO/polyfluorene inorganic/organic hybrid junction. *J. Alloys Compd.*, 2012, **534**(9): 1–5.
- [13] BADRAN R I, UMAR A, AL-HENITI S, *et al.* Synthesis and characterization of zinc oxide nanorods on silicon for the fabrication of p-Si/n-ZnO heterojunction diode. *J. Alloys Compd.*, 2010, **508**(2): 375–379.
- [14] WALTER T, HERBERHOLZ R, MULLER C, *et al.* Determination of defect distributions from admittance measurements and application to Cu(In,Ga)Se₂ based heterojunctions. *J. Appl. Phys.*, 1996, **80**: 4411–4420.
- [15] BOUZITOUN M, DRIDI C, CHAABANE R B, *et al.* Electrical properties of ITO/benzylated cyclodextrins(b-CDs (Bz))/Al diode structures. *Sci. Technol. Adv. Mat.*, 2006, **7**: 772–779.
- [16] MUSSELMAN K P, MARIN A, WISNET A, *et al.* A novel buffering technique for aqueous processing of zinc oxide nanostructures and interfaces. *Adv. Funct. Mater.*, 2011, **21**(3): 573–582.

平面 Si/PCBM 与纳米 Si/PCBM 有机-无机杂化 异质结的对比研究

刘维峰¹, 边继明^{1,2}, 骆瑛琳¹, 乔建坤¹, 赵春一¹

(1. 大连理工大学 三束材料改性教育部重点实验室, 物理与光电工程学院, 大连 116024; 2. 中国科学院特种无机涂层重点实验室, 上海 200050)

摘 要: 本研究采用平面硅与纳米硅分别与旋涂法生长的[6,6]-苯基 C61-丁酸甲酯(PCBM)形成有机-无机杂化异质结, 对比研究了两种异质结界面电学特性的差异。结果显示, 平面 Si/PCBM 和纳米 Si/PCBM 两种异质结都表现出明显的整流特性, 但相对于平面 Si/PCBM 异质结, 纳米 Si/PCBM 异质结有较大的导通电压和较小的电流密度。为了深入研究导致这种差异的相关物理机制, 通过阻抗谱(IS)表征技术进一步研究了两种异质结因界面变化而产生的电阻、电容的变化趋势。阻抗测试分析表明, Si/PCBM 异质结界面存在的大量缺陷致使寄生效应进一步增大, 影响了器件中电荷的输运。

关 键 词: 无机-有机异质结; 纳米 Si/PCBM; 阻抗谱; 瞬态光伏谱

中图分类号: TB34

文献标识码: A